

# Gravitational Flow

Carl S. Reiff  
Loomis, California, USA  
creiff@elgenwave.com

This paper posits that 'Gravitational Flow' permeates the Universe, and all observed time dilation is a result of movement relative to this flow. The speed of the flow at any given location is simply the corresponding escape velocity. So time dilation can be calculated from escape velocities. The procedure is illustrated using three distinct examples: **1)** The time dilation setting required by the atomic clocks aboard the GPS satellites orbiting Earth; **2)** The Shapiro delay experienced by a ray of light as it passes very near the Sun; **3)** The portion of the perihelion precession of Mercury's orbit that is due to time dilation, often called 'anomalous precession'. Also included are proposals for four distinct experiments, each of which will demonstrate the effects of the flow.

## Introduction

The nature of gravity has long been a topic of interest and research. Theories regarding it have varied over time. Newton described gravity as an attractive force. Einstein described it as a curvature of space-time. This paper describes gravity is a flow.

Every particle of matter has a flow that terminates in itself. This flow spans the universe, and wherever it accelerates through any other particle of matter, it exerts a pressure - like a drag. However, the flow itself is unaffected by any matter through which it accelerates. The amount of pressure exerted is directly proportional to the amount of actual matter in matter; *i.e.*, the nuclei and electrons in atoms. Measurements of the amount of empty space surrounding atomic nuclei indicate just how minuscule the actual amount of matter is in physical matter.

When Newton formulated the laws of gravitation, he used a gravitational constant  $G$ . Over a century later, Henry Cavendish constructed a device to measure  $G$ . Over a century after that, Ernest Rutherford devised an experiment that revealed the structure of an atom. The measured value of  $G$  corresponds directly with structure of the atom - or, more specifically, with the minute proportion of the nuclei (and electrons) in all atoms, molecules, compounds and masses. In other words, it is a representation of the mean density of all physical matter in the universe - excepting singularities. The effect that gravitational flow has on matter fits this understanding perfectly. The gravitational flow model also fits perfectly with the very subtle gravitational differences accounted for by time dilation, and since an accounting of time dilation is requisite in any gravitational model, the examples in this paper detail how the concepts of gravitational flow can be used to accurately calculate it.

## Telling Behaviors of Light

Light has many properties, one of which is the perfectly characteristic behavior of light as it passes through various substances, and another of which is how it behaves when it transitions between them. For example, the speed of light ( $c$ ) in the vacuum of space is roughly three million meters per second[1], and in glass it's roughly two million meters per second[2]. When

light transitions from the vacuum of space to glass, it doesn't "slow down." Rather, it instantaneously assumes the "supported speed" of glass, as given by its refractive index. Likewise, when it transitions back to the vacuum of space, it does so instantaneously. This characteristic behavior is perfectly consistent. Light could transition between the vacuum of space to glass, to water, back to glass, to oil, to diamond, and back to the vacuum of space, and it would travel at the precise 'supported speed' of each substance along the way, and each transition would be instantaneous. This perfectly consistent behavior begs the questions: If there isn't anything similarly limiting the speed of light in the vacuum of empty space, then why doesn't it just travel from any point in the universe to any other point instantaneously? Why is its speed so similarly and characteristically limited, as it is when passing through various substances?

Gravitational flow limits the speed of light in the vacuum of empty space, similar to how it's limited when passing through any of the substances previously mentioned. Additionally, the flow can move and accelerate, and it does so in proximity to gravitationally significant masses. For a symmetrically spherical mass, the direction of the prevailing flow is directly toward the center of the mass. The speed of the flow at the surface of the mass is given by the escape velocity at the surface radius. The speed of the flow at any given altitude above the surface is simply the escape velocity at that altitude, as measured from the center of the mass.

This coincides perfectly with the behavior of light in proximity to black holes. At the event horizon, the escape velocity is equal to the vacuum speed of light ( $c$ ). As such, the flow is heading inward at that speed. And since the velocity of light is constrained/limited by the flow, light cannot escape at (or interior to) the event horizon.

To understand how the flow affects light, consider two small space ships (A and B) traveling in series towards a supposedly stationary space station. Also consider what might best be described as an aquarium ship whose height and width are relatively small (perhaps 10 meters in each direction), but whose length is enormous (on the order of tens of thousands of kilome-

ters), also traveling towards the space station, but on a path perpendicular to the path of ships A and B. (See Fig. 1)

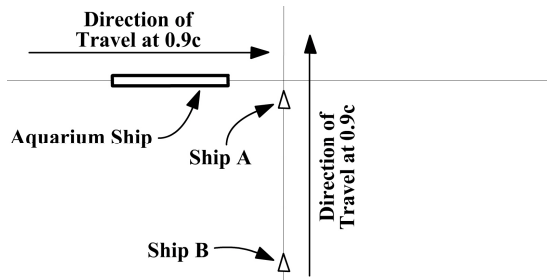


Figure 1. Backward Light Travel before sending signal.

The space station is located at the center of the diagram, and is just a few meters above intersecting paths of the three ships. From there, it sees the distance between itself and ships A and B decreasing at a rate of  $0.9c$ . At a right angle to the path of ships A and B, it also sees the distance between itself and the aquarium ship decreasing at a rate of  $0.9c$ . Ship A wants to send a signal to ship B, but it only has a laser-like, directional broadcasting antenna facing out of its left/port side. When ship A passes directly in front of the oncoming aquarium ship (and under the space station), it sends the signal. (See Fig. 2)

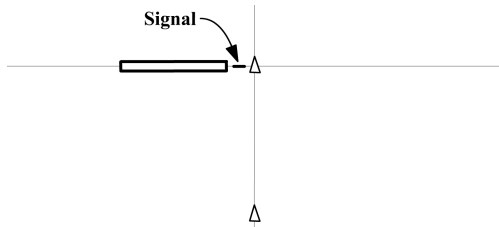


Figure 2. Backward Light Travel - Sending Signal.

Since light is unaffected by the motion of its source, the signal heads straight into the leading end of the oncoming aquarium ship. As the signal enters the water, its speed instantly changes to roughly three-fourths the vacuum speed of light (approximately  $0.75c$ ). [2] However, since the water itself is traveling at  $0.9c$  in the exact opposite direction to the heading of the signal, the signal is actually moving 'backward' at  $0.15c$ . (See Fig. 3)

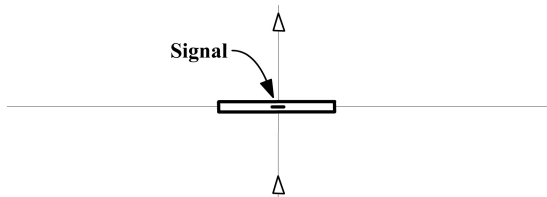


Figure 3: Backward Light Travel - Signal Traveling.

Once the aquarium ship passes out of the path of ship B, the signal passes out of its trailing end, whereupon the signal's velocity instantaneously resumes its original vacuum speed (or  $1.0c$ ). Ship B then passes directly behind the aquarium ship and receives the signal (which arrived from its right/starboard side). (See Fig. 4.)

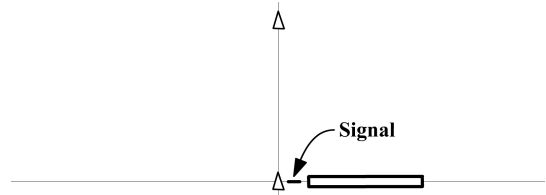


Figure 4: Backward Light Travel - Receiving Signal.

Just as the water limited the speed of the signal, and the movement of the water was faster than the speed of the signal through the water, causing the signal to actually travel 'backward', the speed of the flow interior to the event horizon of a black hole causes even outbound light to travel 'backward' toward the singularity.

## Gravitational Flow Applications

The following Sections present gravitational flow solutions for three relativistic scenarios where the amounts of time dilation are already known. The laws applied are based on the following: 1) The speed of light (in the vacuum of space) is constant relative to the flow; 2) Objects moving relative to the flow experience time dilation. The solutions obtained show how gravitational flow accurately accounts for the time dilations.

### GPS System Time Dilation

Both special and general relativity were used to calculate the total time dilation required for the GPS satellites orbiting Earth. [3] Based on their orbital velocity, special relativity indicated that the clocks aboard the satellites would run slower than ground based clocks by about 7 microseconds per day. [3]

Based on their altitude, general relativity indicated that their clocks would run faster than ground-based clocks by about 45 microseconds per day. [3] The net result was that their clocks needed to be adjusted prior to launch and orbital insertion so that they would run slower than ground based clocks, by about 38 microseconds per day.

The following is a solution for calculating the time dilation of these satellites using escape velocities.

### Set-up Data

Gravitational Constant ( $G$ ):  $6.674 \times 10^{-11} \text{ N}\cdot\text{m}^2 / \text{kg}^2$  [4]

Earth mass ( $M_E$ ):  $5.9736 \times 10^{24} \text{ kg}^2$  [5]

Mean Earth Radius ( $r_{Em}$ ): 6,371 km [5]

Equatorial Earth Radius ( $r_{Ee}$ ): 6,378.1 km [5]

Light Speed ( $c$ ): 299,792,458 m/s [1]

Satellite Altitude ( $A$ ): 20,200 km [6]

Orbital Period ( $P$ ): 43,082.0455 seconds (1/2 sidereal day = 11 hrs, 58 mins, 2.0455 secs) [7].

### Solution

Calculate the escape velocity at the orbital altitude of the satellites ( $v_{esc}$ ):

$$v_{esc} = \sqrt{2GM_E / (r_{Em} + A)} = 5,478 \text{ m/s} \quad (1)$$

Calculate the orbital velocity of the satellites ( $v_{orb}$ ):

$$v_{orb} = 2\pi(r_{Em} + A) / P = 3,875 \text{ m/s} \quad (2)$$

Apply the Pythagorean theorem to obtain their actual velocities relative to the flow ( $v_{act}$ ):

$$v_{act} = \sqrt{v_{esc}^2 + v_{orb}^2} = 6,710 \text{ m/s} \quad (3)$$

Calculate the number of seconds of orbital time dilation ( $\Delta t_{orb}$ ):

$$\Delta t_{orb} = 1 / \sqrt{1 - v_{act}^2 / c^2} - 1 = 2.505 \times 10^{-10} \text{ sec} \quad (4)$$

Calculate the ground escape velocity ( $v_{gesc}$ ):

$$v_{gesc} = \sqrt{2GM_E / r_{Ee}} = 11,181 \text{ m/s} \quad (5)$$

Calculate the rotational velocity of Earth's surface where the ground-based clocks are located. ( $v_{surf}$ ). It is zero at the poles, and reaches a maximum at the equator; this solution assumes an equatorial locale:

$$v_{surf} = \pi r_{Ee} / P = 465 \text{ m/s} \quad (6)$$

Apply the Pythagorean theorem to obtain the actual ground velocity relative to the flow ( $v_{gact}$ ):

$$v_{gact} = \sqrt{v_{gesc}^2 + v_{surf}^2} = 11,191 \text{ m/s} \quad (7)$$

Calculate the number of seconds of ground time dilation ( $\Delta t_{gr}$ ):

$$\Delta t_{gr} = 1 / \sqrt{1 - v_{gact}^2 / c^2} - 1 = 6.967 \times 10^{-10} \text{ sec} \quad (8)$$

Calculate the time dilation difference per sidereal day:

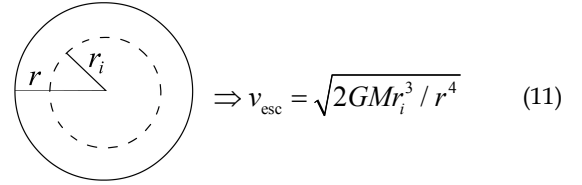
$$2P(\Delta t_{gr} - \Delta t_{orb}) = 3.845 \times 10^{-5} \text{ sec} \quad (9)$$

The time dilation solution works because light rides along with the gravitational flow toward gravitating masses. The rate of the flow at any given distance above the surface of a mass is the corresponding escape velocity ( $v_{esc}$ ) given by:

$$v_{esc} = \sqrt{2GM / r} \quad (10)$$

where  $G$  is the gravitational constant,  $M$  is the mass of the body, and  $r$  is measured from its center.

The flow is also effectual in the interior of spherical masses like stars and planets. Escape velocities ( $v_{esc}$ ) for depths below the surface of a mass (*i.e.*, for radii less than the surface radius) are only dependent on the portion of the mass interior to the chosen radius ( $r_i$ ) as given by:



$$\Rightarrow v_{esc} = \sqrt{2GM_i^3 / r^4} \quad (11)$$

Accordingly, as the flow moves inward from the surface, its velocity decreases, and ultimately reaches zero (0) at the center of the mass. Relative interior and exterior escape velocities (flow rates) for a spherical gravitating mass (Earth in this case) are shown in Fig. 5.

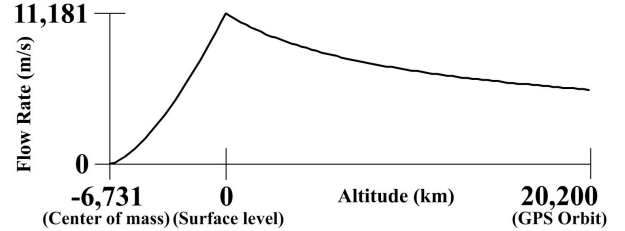


Figure 5. Spherical Mass Flow Rates.

The GPS time dilation solution given above accounts for the gravitational acceleration of the flow at the altitude of the satellites, derived from the escape velocity, and the transverse motion of the satellites through the flow along their orbital path. These two effects are combined to obtain a composite value for the satellites. A simple analogy is the scroll of paper on a player piano. (See Fig. 6)

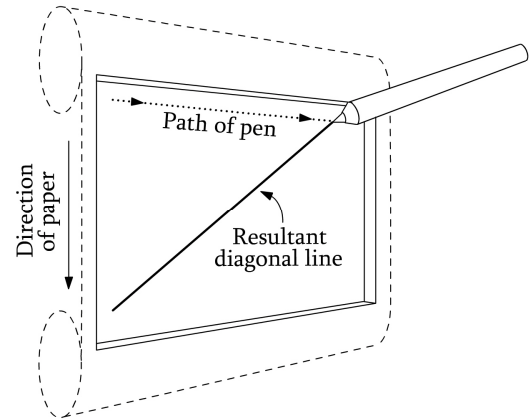


Figure 6: Piano Player Scroll Analogy.

If a pen is used to slowly draw a straight, horizontal line (at a steady rate) across the paper while the paper is moving downward, the resulting line would be diagonal. The paper moving downward represents the gravitational flow, and the motion of the pen moving across the paper represents the orbital path of the satellites. The resulting diagonal line represents the actual path (and distance) traveled by the satellites relative to the flow. This is why the Pythagorean theorem is used in Eq. (3) of the solution.

The piano scroll analogy also applies to the ground based clocks, which is why the calculation steps for them are identical to those for the satellites. The principle of using escape velocities to calculate time dilation also applies in deep space, far from any

gravitating masses. However, in such locales the flow is glacial (*i.e.*, very near zero), so their effect becomes negligible.

### The Shapiro Delay

In the 1960's, Irwin Shapiro conceived and conducted a test of general relativity relating to the delay of a ray of light as it passed near the Sun.[8] The treatment herein applies the principles of gravitational flow to Shapiro's experiment.

Consider a space probe flying along the path of Earth's orbit on the far side of the Sun (as seen from Earth). The orbital position of the probe with respect to Sun and Earth would require that a ray of light sent from Earth to the probe (and back) pass near the surface of the Sun. Since the two legs of the trip are mirror images of each other, only one is addressed herein. Fig. 7 shows the general layout of the test. Some elements of the Figure are exaggerated for readability.

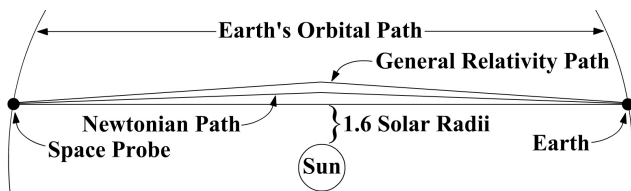


Figure 7. Shapiro Delay Test Setup.

As the light commences its journey from the probe to Earth, gravitational flow towards the Sun begins to increase, causing the speed of the light to equally increase (relative to the Sun) as well. The closer the light gets to the Sun, the faster the flow, so the faster the light's speed, until about the 45 degree mark (along the path of the light relative to the center of the Sun), where the 'tailwind' becomes more of a crosswind. (See Fig. 8) From this point, the light's forward velocity begins to decline as the flow is moving more transverse to it. At the 90 degree mark (as the light makes its closest approach to the Sun), it's a full on crosswind, and the light continues to slow as it starts to experience a little bit of a headwind. By about the 135 degree mark, the crosswind becomes more of a headwind, but the rate of this headwind diminishes as the light moves further away from the Sun. As it does, its speed increases.

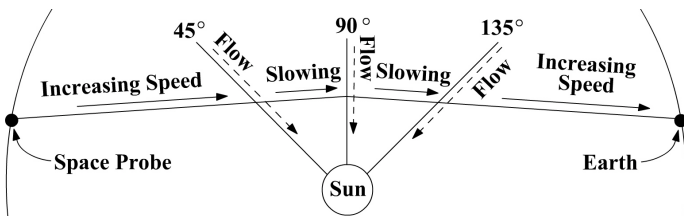


Figure 8. Flow-affected speed of light.

Although the light picks up speed from the tailwind on its way in, and then loses speed due to the headwind on the way out, these two segments of the journey do not simply cancel each other out. The reason is that although the sum of both the headwind and tailwind do equal each other, the light spends more time fighting through the headwind, than it spends being boosted by the tailwind. Consequently, the light ray is delayed, and the total travel time is therefore increased.

Using general relativity, Shapiro showed that the maximum delay a ray of light would experience passing near the surface of the Sun would be 240 microseconds for a round trip (or 120 microseconds in each direction).[9] Of course, with the intense amount of interference that close to the Sun's surface, it would be extremely unlikely that a discernible signal would make it through. However, at an altitude of 1.6 solar radii, a recognizable signal can get through. At that altitude, Shapiro showed that general relativity predicts a one way delay of 100 microseconds.[8] Shapiro's testing later confirmed the 100 microsecond delay for each leg of the round trip.[10]

Computer software was used to perform the gravitational flow based calculations for the Shapiro delay, and to run simulations thereof. The simulations agreed with a maximum 240 microsecond round trip delay when grazing the surface of the Sun, and duplicated the 100 microsecond one way delay at 1.6 solar radii above Sun's surface.

### Shapiro Delay Computer Simulation Methodology

The software for the computer simulations was designed to mimic and account for the motions of the flow along the path followed by the ray of light. At a distance of roughly 150,000,000 km away from the Sun (*i.e.*, the orbit distance of Earth), the probe sends a signal that will pass near the Sun on its way to Earth. As the light ray is expected to pass by the Sun at 1.6 solar radii above the surface, its initial trajectory is at a slight angle relative to the Sun's center; *i.e.*, the direction to where the flow is heading.

The software split the overall trip into tens of thousands of small segments, minutely calculating and summing the effects of the flow throughout the trip. In the early part of the trip, the flow rate is relatively low, so the amount of heading deviation experienced by the light ray is minimal. (See Fig. 9.) Note that some of the portions and angles depicted in Figs. 9-12 are exaggerated for clarity.)

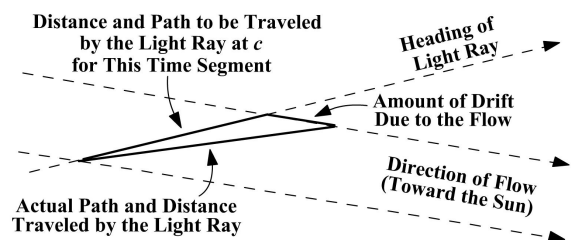


Figure 9. Shapiro Delay Test Methodology - Early Segment.

Figure 10 shows a small series of the segments depicted in Fig. 9. Its purpose is to imbue a sense of the cyclical processing nature that the software utilized in performing the billions of minutely detailed trigonometric calculations when executing the simulations.

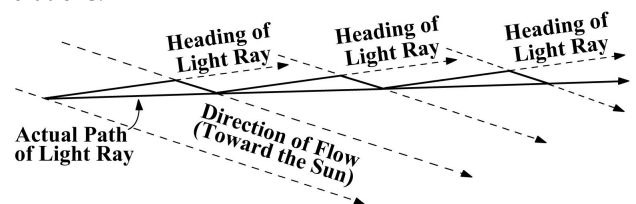


Figure 10. Shapiro Delay Test Methodology - Early Segment Series

As the light ray nears the Sun, the rate of the flow is much greater, and its relative direction is much more transverse. (See Fig. 11)

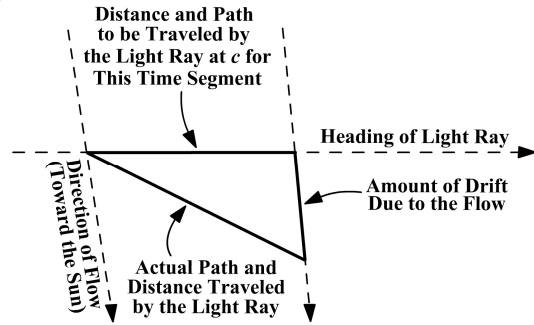


Figure 11: Shapiro Delay Test Methodology - Early-mid Segment.

After the light ray passes the Sun and begins to move away, the flow begins to work against it, retarding its progress. (See Fig. 12)

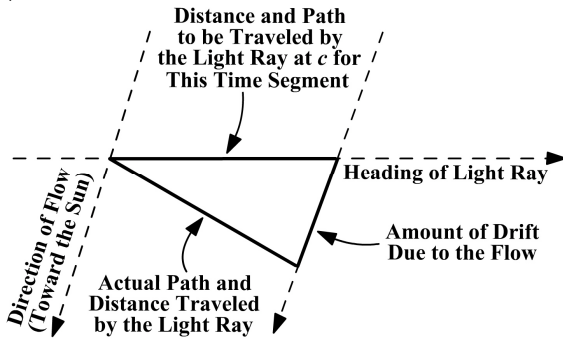


Figure 12: Shapiro Delay Test Methodology - Late-mid Segment.

As the light ray approaches Earth, the flow becomes much more of a direct headwind. However, because of being so far from the Sun, the rate of the flow is significantly reduced, causing the rate of progress made by the light ray to increase. (See Fig. 13)

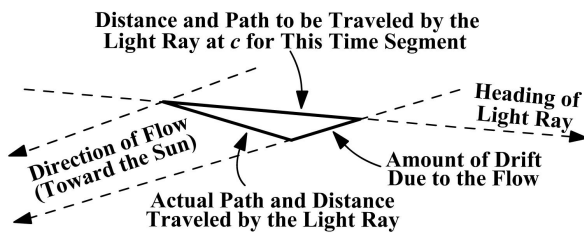


Figure 13: Shapiro Delay Test Methodology - Late Segment

The calculated data produced by the simulations provided crucial insights into just how dramatic the effects of the flow are regarding light. While the paths of the light rays for the Newtonian and general relativity predictions are both straight lines, each with a very slight bend in the middle, the simulation data show a very different path for the flow affected light ray. Additionally, while the inbound (toward the Sun) and outbound (away from the Sun) legs of both the Newtonian and general relativity predicated paths are symmetric mirror images of each other, the inbound and outbound legs of the flow-affected path are rather asymmetric. This is not to say that the appearance of the path for an Earth-bound observer is in any respect different

from the general relativity predicted path. Rather, they would seem identical. After all, all that is known by an observer (as the light ray enters his eye), is the tangent of the line (or curve) at that point. The tangent only provides a perceived path, and/or point of origin. The actual path is not necessarily the same, especially when vast distances are involved.

Fig. 14 shows a graph of the path followed by the light ray - from the space probe to Earth. The graph is compressed horizontally (from left to right), that's why the Sun is depicted as a thin vertical line.

General relativity predicts a deflection of 1.75 seconds of arc.[11] Even over the roughly 300,000,000 kilometer distance, the total height above the straight line at the midpoint between the space probe and Earth is only about 1,300 (thirteen hundred) kilometers, while the apogee of the flow affected path (per the simulation data) is more than 8,700 (eighty-seven hundred) kilometers.

The height of the flow-affected path depicted in Fig. 14 is exaggerated by a factor of 5 for emphasis. The steep dive at the midpoint of the path is due to the dramatically increased rate of the flow near the Sun.

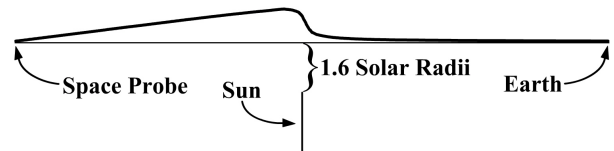


Figure 14: Shapiro Delay - Flow Affected Light Path

The simulation data also shows that of the total 100 microsecond delay, only 10 microseconds are actually due to the light ray spending more time fighting against the headwind of the flow on its way out from the Sun, as opposed to the time spent being boosted by the flow on the way in. The other 90 microseconds are purely a result of the longer path traveled.

### The Perihelion Precession of Mercury's Orbit

For several decades astronomers were perplexed by a portion of the perihelion precession of Mercury's orbit for which they could not account.[12] Using General Relativity Theory (GRT), Einstein was able to accurately calculate it - as it was due to time dilation.[12] It turns out that the orbits of all celestial bodies in the solar system precess, and at least a portion of all those precessions is similarly due to time dilation.

Gravitational Flow also accurately accounts for the time dilated portions of the orbits of all celestial bodies in the solar system. For perfectly circular orbits, the method for calculating the time dilation is largely synonymous with that of the GPS satellites as given in Eqs. (1-4). The sole difference for elliptical orbits has to do with the fact that the altitude (distance from the Sun) increases during the outbound half of the orbit - from perihelion to aphelion, and then decreases during the inbound half of the orbit - from aphelion to perihelion. Therefore, a slightly modified piano scroll analogy is needed. Fig. 15 depicts a radial view of how a planet in an elliptical orbit increases its altitude (distance from the Sun) during a one-second interval as it travels along the outbound half of its orbit.

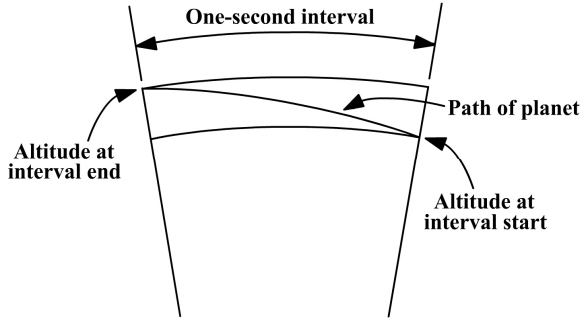


Figure 15: Radial Orbital Ascension.

For elliptical orbits, the flow rates and other parameters are constantly changing throughout the orbital period. Therefore, computer software was used to model Mercury's orbit, and to divide it into equally sized segments using Kepler's 2<sup>nd</sup> law of planetary motion.[13] During the orbital simulation, the software calculated and summed the time dilation (for both the outbound and inbound halves of the orbit) from each of the more than 7.6 million one-second time intervals. The segments were 'rectangularized' similar to those of the GPS satellites presented earlier. Figures 16 and 17 use this format for the outbound and inbound segments respectively. Note: Fig. 16 is the rectangularized equivalent of the radial view shown in Fig. 15.

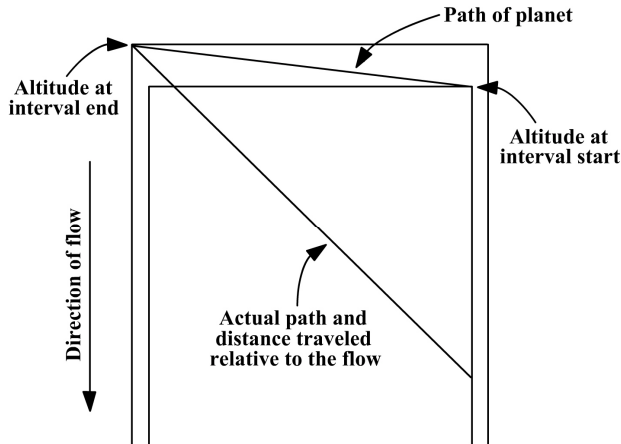


Figure 16: Outbound Flow Path.

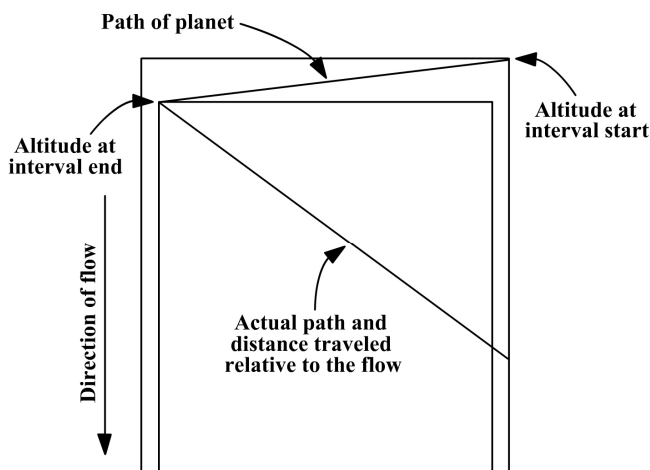


Figure 17: Inbound Flow Path.

Just as the higher altitude radial segment in Fig. 15 is longer than the lower altitude one, the higher altitude rectangularized segments in Figs. 16 and 17 are also longer. In Fig. 16, the orbital path of the planet initiates at the 'right' end of the narrower, lower altitude segment, and concludes at the 'left' end of the wider, higher altitude segment. Accordingly, the line representing the orbital path of the planet does not span the entire width of the higher altitude segment, a key point that is not as directly elucidated in the radial view of Fig. 15. Fig. 17 shows the inbound equivalent of Fig. 16. The key difference between the two lies in the lengths of the 'actual path' lines, which are the respective distances traveled relative to the flow. The outbound 'actual path' line (in Fig. 16) is longer because it passes through more of the flow as the planet moves further away from the Sun. Conversely, the inbound 'actual path' line (in Fig. 17) is shorter because the planet moves with the flow as it approaches the Sun.

When calculating the amount of time dilation for each one-second interval, the software uses the escape velocity at the altitude halfway between the starting and ending segment altitudes. It then employs the Pythagorean theorem (using both the 'horizontal' distance traveled by the planet and the amount of 'vertical' flow which passed through the planet during the interval) to calculate the actual amount of flow traversed. For outbound intervals, it factors in the increase in altitude. This is what makes the diagonal flow line longer in Fig. 16. For inbound intervals, it factors in the decrease in altitude. This is what makes the diagonal flow line shorter in Fig. 17. The software then calculates the amount of time dilation based on the total amount of flow which passed through the planet during the interval. The time dilation for all the outbound and inbound intervals are summed, resulting in values for the total outbound time dilation ( $\Delta t_{out}$ ), and the total inbound time dilation ( $\Delta t_{in}$ ). The total amount of time dilation ( $\Delta t_{tot}$ ) experienced by the planet during one orbit is then given by:

$$\Delta t_{tot} = (\Delta t_{out} + \Delta t_{in}) \left[ \sqrt{\Delta t_{out} / \Delta t_{in}} + (\Delta t_{out} / \Delta t_{in})^2 \right] \quad (12)$$

The summed outbound and inbound time dilation values for Mercury are  $\Delta t_{tot} = 0.163401$  and  $\Delta t_{in} = 0.127325$ . Plugging these values into Eq. (12) yields a total orbital time dilation of  $\Delta t_{tot} = 0.80816$  seconds, which is measured from the aphelion along the circumference of the perfect circle equivalent of Mercury's elliptical orbit.

Elliptical orbits have several properties. Examples are aphelion, perihelion, major axis, minor axis, eccentricity, circumference, area and period. One of these properties is constant for any given orbit, regardless of any other factor: the aphelion. In other words, if Mercury's orbit was either more or less eccentric, it's aphelion distance would still be exactly the same as it is now. And, if its orbit were a perfect circle, the radius thereof would match its current aphelion distance exactly.

The number of arcseconds of precession in Mercury's orbit during one Earth century is:

$$t \times n_0 \Delta t_{tot} / a = 43.22 \text{ arcsec} \quad (13)$$

where  $t$  is the number of arcseconds in a full circle (or  $360 \times 60 \times 60$ ),  $n_0$  is the number of Mercury orbits in one Earth century (or  $365.256^{[14]} \times 100 \div 87.9691$  [15]),  $\Delta t_{tot}$  is the total orbital time dilation given above (*i.e.*, 0.80816), and  $a$  is the number of seconds contained in a perfectly circular orbit whose radius is equal to Mercury's aphelion distance.

Use of the software was not limited to Mercury; it was also employed to calculate the precession of other celestial bodies. Table 1 in Appendix A contains the time dilation values for the four inner planets (Mercury, Venus, Earth and Mars) and the asteroid Icarus.

Extensive analysis of the data from the software runs for the various planets revealed a pattern. This pattern provided the key allowing orbital precession values to be calculated by hand, obviating the use of computer software.

### A Minimalist Method

Every one-second interval throughout any elliptical orbit is unique with respect to the amount of time dilation experienced therein. The orbital time dilation formula in Eq. (12) operates on the total amounts of time dilation experienced on both the outbound and inbound halves of the orbit. As such, it follows that if the one-second intervals with the average amounts of time dilation could be determined for each side of the orbit, then multiplying them by half the period (in terms of seconds) would yield the two values required in Eq. (12).

Figure 18 shows an elliptical orbit, along with its perfect circle equivalent as given by their shared aphelion distance. The aphelion line extends vertically from the dot representing the Sun at the center of the diagram. Just to the left of the aphelion line is another line (the 'theta line'), also extending from the Sun, and separated from the aphelion line by a certain angle ( $\theta$ ).

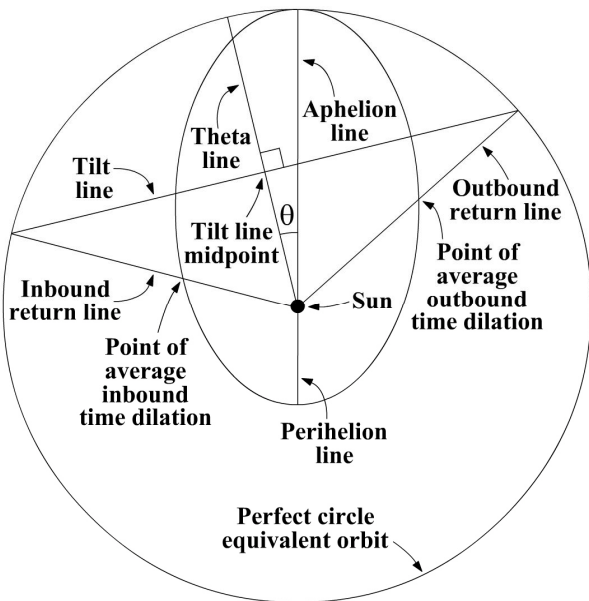


Figure 18: Average Time Dilation Points.

Perpendicular to the theta line is the 'tilt line', which extends to the equivalent circular orbit at its ends, and which intersects the theta line at a certain distance from the Sun. The distance is calculated by applying a factor (a percentage) to the aphelion

distance. The point where the theta line intersects the tilt line is the midpoint of the tilt line. For various orbital eccentricities, table 2 in Appendix A lists the corresponding angles and factors. Polynomial curve fitting can be employed to determine the values pertaining to any eccentricity.

There are two other lines in Fig. 18: the outbound and inbound return lines. They start at either end of the tilt line, and extend back to the Sun. The points where they intersect the elliptical orbit are the locations of average time dilation.

Because this minimalist method requires multiplying the average outbound and inbound time dilation factors by several millions (*i.e.*, by half the orbital period in terms of seconds), the orbital parameters need to be extremely precise. Given only the aphelion and perihelion distances, all other orbital parameters can be derived. Unfortunately, the astronomical measurements for these values lack the requisite precision for the task at hand.

Unlike most astronomical measurements, the period of a planet is one whose precision increases with time since it is the average of an ever-increasing number of continuous orbits. The strict formulaic relationship between the period of a planet and its aphelion and perihelion distances (via the semi-major axis) can be used to check the measurements. For example, the period of a planet (in terms of seconds) can be calculated from the aphelion and perihelion distances, as given in Kepler's third law:

$$T = \sqrt{4\pi^2 r^3 / GM} \quad (14)$$

where  $r$  is the semi-major axis [*i.e.*, (aphelion + perihelion)  $\div$  2]. If the period thus calculated does not equal the observed period, then the measured distances aren't merely inaccurate, they're definitionally wrong.

To understand how the successively continuous nature of planetary orbits allows their period measurements to be refined over time, consider a planetary orbit where the date and time of its perihelion occurrence is recorded, with an accuracy of plus or minus 62.0 seconds. One orbit later, the date and time of the next perihelion occurrence is likewise recorded, also with an accuracy of plus or minus 62.0 seconds. Thus, the period measurement has an overall accuracy of plus or minus 124 seconds. However, since orbits are successively continuous, the date and time of each successive perihelion occurrence can be likewise recorded (all plus or minus 62.0 seconds) and measured against the first recorded date and time. If the planet's period was 88 Earth days, then, after one Earth century (or 415 subject planet orbits), the period accuracy would be increased to plus or minus  $124 \div 415 = 0.3$  seconds.

In cases where the period calculated from the aphelion and perihelion doesn't match the observed period, the incongruity can be remedied by adjusting the aphelion and perihelion distances by the ratio of the observed period divided by the calculated period. Thereby, the aphelion and perihelion distances can be brought into conformity with the observed period. All perihelion precession computations herein employ these adjustments when the calculated periods don't match the observed periods

Through this minimalist method, the portion of Mercury's orbital precession which is due to time dilation can be calculated

by first looking up (or determining via polynomial curve fitting) the angle of the theta line, and the distance factor for the tilt line (based on Mercury's eccentricity) from Table 2 in Appendix A. Doing so yields an angle of 13.676040459 degrees, and a factor of 0.1664724963.

The following minimalist method solution utilizes boundary calculations. See Appendix B for an explanation of this process.

### Set-up Data

Mass of Sun  $M = 1.9891 \times 10^{30}$  [15]

Gravitational constant  $G = 6.6726 \times 10^{-11}$  [4]

Angle of tilt ( $a_{lt}$ ): 13.676040459 degrees

Offset factor ( $f_{off}$ ): 0.1664724963

Adjusted aphelion length ( $a_{adj}$ ) = 69,820,150,084 meters

Adjusted perihelion length ( $p_{adj}$ ) = 46,003,341,427 meters

Orbit period (seconds)  $T = 7,600,530$  seconds [15]

Segment size (orbital area /  $T$ )  $s_{area} = 1,356,618,483,573,281$  m<sup>2</sup>

Speed of light  $c = 299,792,458$  m/s [1]

### Solution

Calculate the distance between the Sun and the tilt line ( $l$ ):

$$l = a_{adj} \times f_{off} = 11,623,134,677 \text{ meters} \quad (15)$$

Calculate the angle between the outbound return line and the perihelion line (as measured counter-clockwise from the perihelion) ( $a_{pout}$ ):

$$a_{pout} = 180 - \left[ 90 - \sin^{-1}(l / a_{adj}) \right] = 113.25909 \text{ deg} \quad (16)$$

Determine the distance between the Sun and the point of average outbound time dilation ( $l_{out}$ ). This requires an iterative process that utilizes the principle that any point along an elliptical orbit can be located by using a triangle where two of its corners are located at the two foci, and the sum of the lengths of its sides is twice the aphelion distance. The full iterative process won't be shown here, but the result is:

$$l_{out} = 60,364,706,689.6434 \text{ meters} \quad (17)$$

Calculate the rectangularized width of this one-second segment ( $w_{out}$ ):

$$w_{out} = 2s_{area} / l_{out} = 44,947 \text{ meters} \quad (18)$$

Use the Pythagorean theorem to calculate the length of the hypotenuse through half the width of this segment ( $h_{out}$ ):

$$h_{out} = \sqrt{s_{area}^2 + (w_{out} / 2)^2} = 60,364,706,689.6476 \text{ meters} \quad (19)$$

Calculate the angle between the outbound return line and hypotenuse line ( $a_{out}$ ):

$$a_{out} = \sin^{-1}(w_{out} / 2) / h_{out} = 2.133115 \times 10^{-5} \text{ deg} \quad (20)$$

Calculate the lengths of the long ( $l_2$ ) and short ( $l_3$ ) sides of the segment. These require the same iterative process used previously for  $l_{out}$  in Eq. (17):

$$l_2 = 60,364,711,311 \text{ meters} \quad (21)$$

$$l_3 = 60,364,702,069 \text{ meters} \quad (22)$$

Calculate the width of the segment at the short side distance ( $w_2$ ):

$$w_2 = 2 \times l_3 \times \sin a_{out} = 44,947.4024 \text{ meters} \quad (23)$$

Calculate the width of the segment at the long side distance ( $w_3$ ):

$$w_3 = 2 \times l_2 \times \sin a_{out} = 44,947.4092 \text{ meters} \quad (24)$$

Calculate the length difference between the short and long sides of the segment ( $l_4$ ). This is the total increase in altitude (distance from the Sun) during the one-second interval:

$$l_4 = l_2 - l_3 = 9,242 \text{ meters} \quad (25)$$

Calculate the escape velocity at the average distance for this interval ( $v_{esc}$ ):

$$v_{esc} = \sqrt{2GM / l_{out}} = 66,313 \text{ m/s} \quad (26)$$

Calculate the total vertical flow passing through Mercury during the interval ( $f_{out}$ ):

$$f_{out} = v_{esc} + l_4 = 75,555 \text{ m/s} \quad (27)$$

Calculate the length of the actual diagonal path through the flow that Mercury travels during the interval ( $l_5$ ):

$$l_5 = \sqrt{f_{out}^2 + [w_2 + (w_3 - w_2) / 2]^2} = 87,914 \text{ meters} \quad (28)$$

Calculate the amount of time dilation experienced by Mercury during this interval ( $\Delta t_2$ ):

$$\Delta t_2 = \left[ 1 / \sqrt{1 - (l_5 / c)^2} \right] - 1 = 4.2997348 \times 10^{-8} \text{ sec} \quad (29)$$

Calculate the total time dilation for the outbound half of the orbit ( $\Delta t_{out}$ ):

$$\Delta t_{out} = \Delta t_2 T / 2 = 0.1634013178 \text{ sec} \quad (30)$$

For the inbound side of the orbit, calculate the angle between the inbound return line and the perihelion line (as measured clockwise from the perihelion) ( $a_{pin}$ ):

$$a_{pin} = 180 - \left[ 90 + \sin^{-1}(l / a_{adj}) \right] = 85.90648 \text{ deg} \quad (31)$$



Determine the distance between the Sun and the point of average outbound time dilation ( $l_{in}$ ). This requires the same iterative process used previously for  $l_{out}$  in Eq. (17):

$$l_{in} = 54,660,663,374.3154 \text{ meters} \quad (32)$$

Calculate the rectangularized width of this one-second segment ( $w_{in}$ ):

$$w_{in} = 2s_{area} / l_{in} = 49,638 \text{ meters} \quad (33)$$

Use the Pythagorean theorem to calculate the length of the hypotenuse through half the width of this segment ( $h_{in}$ ):

$$h_{in} = \sqrt{s_{area}^2 + (w_{in} / 2)^2} = 54,660,663,374.3210 \text{ meters} \quad (34)$$

Calculate the angle between the inbound return line and hypotenuse line ( $a_{in}$ ):

$$a_{in} = \sin^{-1}(w_{in} / 2) / h_{in} = 2.601540 \times 10^{-5} \text{ deg} \quad (35)$$

Calculate the lengths of the long ( $l_6$ ) and short ( $l_7$ ) sides of the segment. These require the same iterative process used previously for  $l_{out}$  in Eq. (17):

$$l_6 = 54,660,668,391 \text{ meters} \quad (36)$$

$$l_7 = 54,660,658,357 \text{ meters} \quad (37)$$

Calculate the width of the segment at the short side distance ( $w_4$ ):

$$w_4 = 2 \times l_7 \times \sin a_{in} = 49,637.8300 \text{ meters} \quad (38)$$

Calculate the width of the segment at the long side distance ( $w_5$ ):

$$w_5 = 2 \times l_6 \times \sin a_{in} = 49,637.8391 \text{ meters} \quad (39)$$

Calculate the length difference between the short and long sides of the segment ( $l_8$ ). This is the total decrease in altitude (distance from the Sun) during this one-second interval:

$$l_8 = l_6 - l_7 = 10,033 \text{ meters} \quad (40)$$

Calculate the escape velocity at the average distance for this interval ( $v_{in}$ ):

$$v_{in} = \sqrt{2GM / l_{in}} = 69,687 \text{ m/s} \quad (41)$$

Calculate the total vertical flow passing through Mercury during the interval ( $f_{in}$ ):

$$f_{in} = v_{in} - l_8 = 59,654 \text{ m/s} \quad (42)$$

Calculate the length of the actual diagonal path through the flow that Mercury travels during the interval ( $l_9$ ):

$$l_9 = \sqrt{f_{in}^2 + [w_4 + (w_5 - w_4) / 2]^2} = 77,605 \text{ meters} \quad (43)$$

Calculate the amount of time dilation experienced by Mercury during this interval ( $\Delta t_3$ ):

$$\Delta t_3 = \left[ 1 / \sqrt{1 - (l_9 / c)^2} \right] - 1 = 3.3504455 \times 10^{-8} \text{ seconds} \quad (44)$$

Calculate the total time dilation for the inbound half of the orbit ( $\Delta t_{in}$ ):

$$\Delta t_{in} = \Delta t_3 T / 2 = 0.1273258093 \text{ seconds} \quad (45)$$

Plugging the total outbound ( $\Delta t_{out}$ ) and inbound ( $\Delta t_{in}$ ) time dilation amounts into Eq. (12) yields 0.80816 seconds of time dilation per orbit of Mercury. Converting to arcseconds per Earth century yields 43.22, as is given in Eq. (13).

The process for calculating time dilation for perfectly circular orbits is virtually identical to that of the GPS satellites shown earlier. Since there aren't outbound and inbound sides to such orbits, any one-second interval can be chosen, as all intervals are identical. The time dilation value for that one interval would then be multiplied by the number of seconds in the entire period of the planet, rather than just half, in order to produce the total value ( $d$ ). In such cases, Eq. (12) reduces to:

$$\Delta t_{tot} = 2d \quad (46)$$

Accordingly, any planet in a perfectly circular orbit would also experience precession due to time dilation. However, since the orbit wouldn't have a perihelion to use as a reference point, the precession just wouldn't be observable.

### Behavior Near Black Holes

At the event horizon of a black hole, the flow reaches the speed of light, and since the speed of light is constant relative to the flow, light emitted interior to the event horizon cannot escape. Additionally, the event horizon is not necessarily where time dilation reaches its zenith. Neither are objects interior to the event horizon necessarily more time dilated than those exterior to it, as time dilation occurs only when objects are in motion relative to the local flow.

As such, an object accelerated to  $0.9c$  relative to the flow, in the direction of a black hole, will cross the event horizon at  $1.9c$  (relative to the singularity), but its time dilation will correspond exclusively to its  $0.9c$  speed relative to the flow. And since all time dilation is measured with respect to motion relative to the flow, an object that is motionless relative to the flow will experience no time dilation as it falls into a black hole.

Because of time dilation, a rocket ship could not accelerate to the speed of light relative to the flow. As the ship approaches  $c$ , time dilation begins to degrade the effectiveness of its engines. The faster it goes, the more they're degraded. It's like placing a penny on a floor, and then moving it halfway toward a wall, and then moving it halfway again, and so on. In doing so, the penny

will forever be approaching the wall, but it won't ever actually reach it.

Additionally, no rocket ship would be able to hold a position just outside the event horizon of (or anywhere relatively near) a black hole. Due to time dilation, the effectiveness of its engines would be so degraded that it would plummet in.

**Motion**

All motion (not just uniform motion) is absolute, because it's measured against the flow. In deep space, far from any gravitational masses, the rate of the flow is very near zero. As a gravitational mass is approached, the velocity of the flow increases - the larger the mass, the larger the increase.

If a space ship is traveling at some fixed velocity relative to the flow - say 5,000 meters per second, it will continue at that velocity - relative to the flow - unless acted upon by some force, as in the case of firing its engines. Even if the flow accelerates - as when nearing a gravitating mass, the space ship will constantly maintain its 5,000 m/s differential relative to the flow - without "feeling" any sense of the flow's acceleration.

Consider two space ships (A and B) separated by some distance, both traveling at 5,000 m/s relative to the flow, and both on a line with, and heading toward a gravitating mass with ship A nearer the mass. As the ships approach the mass, the flow accelerates toward it. Therefore, the ships also accelerate relative to the mass. However, even though their velocity relative to the flow remains constant (at 5,000 m/s), the distance between the ships increases. This is simply a result of the flow local to ship A accelerating faster than the flow local to ship B. And the reason it occurs is because the flow velocity at any given distance from a gravitating mass is simply the corresponding escape velocity.

**Rest and Accelerating States**

Any object that is not in a state of acceleration relative to the local flow is defined as being in a state of rest relative to the flow. Being at rest relative to the flow does not necessarily mean being motionless relative to the flow. In fact, the motionless rest state is a special case. It is the only state - rest or accelerating - where time dilation does not occur. This is true, even for an object falling into a black hole. Time dilation is measured solely relative to the local flow. This holds regardless of the flow's local motion (or lack thereof) relative to the cosmos.

An object at rest on the surface of Earth is not at rest relative to the flow. Even though its velocity relative to the flow is constant, the flow is, in actuality, accelerating through it. This is what causes the 'feeling' of gravity. It doesn't matter whether an object is accelerating relative to the flow, or the flow is accelerating relative to an object, the result is a 'feeling' of gravity.

**Red-shift**

The red-shift of light, whether from a massive star, or a star that is rapidly moving (away from Earth) is accounted for by the flow. While the reasons for the red-shift in each case differ, the result is the same. In the case of a rapidly moving star, the light waves emitted become elongated due to the Doppler effect. The situation is synonymous with a race car speeding along at a constant velocity. Figure 19 represents a race car moving at half the

speed of sound. The cadence of the detonations in the piston chambers is constant, and is indicated by the dots. The sound of each detonation is propagated both forward and backward at the maximum velocity supported by the medium - the atmosphere in this case, and is indicated by the parens. The time coordinate is vertical, and flows from top to bottom. Movement of the race car is horizontal - from left to right.

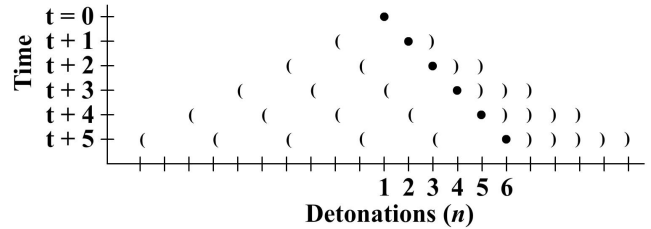


Figure 19. Frequency Shifted Wave Propagation.

The arrangement of Fig. 19 is also applicable to a star moving at half the speed of light. The successive wave fronts bunch up (compress) in front of the star, in the direction of its motion - causing the light to shift toward the blue end of the spectrum, while they spread out (elongate) behind it, causing the light to shift toward the red end of the spectrum.

For a massive star, the red-shift is due to the waves of the emitted light expanding (lengthening out) as they move away from the star. This happens because the rate of the flow is very rapid at the surface of the star, and gradually decreases with distance. The effect is actually very similar to the Doppler effect described above in relation to Fig. 19. The only difference is that the rate of rapidity isn't uniform. Rather, it's accelerated. Or, more accurately, it's accelerating. Specifically, as the flow approaches the star, its velocity increases. The closer it gets, the more its velocity increases, as it's velocity at any given point (altitude) is simply the corresponding escape velocity.

Figure 20 shows a light ray as it moves away from a massive star. The hash marks along the path of the ray represent equal time segments. In other words, the length of time it takes for the light ray to travel between any two hash marks is the same. As such (i.e., because of the way the waves gradually elongate), it might possibly best be referred to as a gradient Doppler effect.

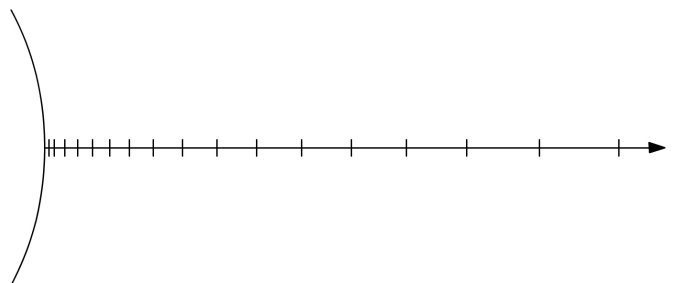


Figure 20: Gradient Frequency Shifted Wave Propagation

**Additional Tests**

While it is true that no experiment can be performed to distinguish between gravitational acceleration and non-gravitational acceleration using inertial materials, such is not the

case with light. Light is rather unique in that it is massless and, therefore, has no inertia. This is why it instantly changes speed as it passes from one substance to another. This is also why it always travels at the highest supported speed of any given substance.

### Gravitational vs. Non-gravitational Acceleration

Gravitational acceleration is a state of acceleration where a change in velocity (for an object) does not occur. This is the case for objects sitting on the surface of Earth. Although they are constantly in a state of acceleration, they are not accelerating. Their velocities are constant, because their velocities (relative to the flow) are simply their escape velocities. All other acceleration, regardless of whether it occurs in a gravitational field, involves constantly changing velocity. All motion is measured relative to the local flow, and all motion relative to the local flow results in time dilation, and any movement of the flow relative to the cosmos is irrelevant with respect to time dilation.

Although the 1g of acceleration experienced by an object at rest on the surface of Earth, and the acceleration experienced by the same object in a space ship accelerating at 1g in deep space are the same, the two can be distinguished via interferometers. For an interferometer at rest on Earth's surface, the flow though occurs at a constant rate. Therefore, it would show a fixed interference/fringe pattern. However, since the velocity of an accelerating space ship is constantly changing relative to the flow, the interferometer would show a constantly changing interference/fringe pattern.

When Michelson and Morley set out to perform their most famous experiment, they designed it based on scientifically sound principles. Their aim was to detect the "aether wind." [16] At the time, the aether was thought to be both ubiquitous and static. [16] As such, Earth would move through it on its orbital path around the Sun.

Thinking the aether was static, they decided to orient their interferometer horizontally on a stone slab floated in mercury so it could be rotated smoothly. [17] Combining this flexibility with the rotation of Earth about its axis would allow their device to "look" in all directions over the period of a day. Michelson and Morley were on the right track, but their experimentation (and that of subsequent researchers) suffered from one fatal flaw.

The flaw laid in the fact that the flow is perpendicular to Earth's surface. Operating under the incorrect premise that the aether was static, they never pointed their interferometer upward. So no matter how they turned their device, or how much Earth rotated, their device was always oriented 90 degrees out of phase. Thus, they unwittingly guaranteed themselves the null result.

If the orientation of the interferometer were changed from the horizontal plane to a vertical one, then as the device is rotated from pointing in the horizontal direction to the vertical direction, the interference pattern (or the fringes thereof) will change.

Appendix C lists an example set of calculations for the Michelson-Morley experiment, and specifies the comparative sensitivity required to perform a synonymous experiment regarding gravitational flow.

### Measuring Flow Affected Light Speed via GPS

A relatively simple test of the effect of the flow on light should be feasible by having the GPS satellites and ground stations send simultaneous signals to each other. Since the clocks of the satellites and ground stations are synchronized, [6] simultaneity of these events shouldn't be an issue.

At a pre-determined time, when a satellite passes directly over a ground station, have both the satellite and the ground station send signals to each other, and have them record the respective times when the signals arrive. Due to the effects of the flow on the travel time of the signals, it will be determined that the signal which traveled down exceeded the speed of light, arriving 1.65 microseconds ( $1.65 \times 10^{-6}$  seconds) sooner, because the flow boosted its speed. Conversely, it will also be determined that the signal that traveled up did so at less than the speed of light, arriving 1.65 microseconds ( $1.65 \times 10^{-6}$  seconds) later, because the flow retarded its speed.

Again, like with the Shapiro delay, a computer simulation was used to calculate these differences. The methodology applied was similar with respect to the headwinds/tailwinds, but differed in that this simulation didn't involve or require the computation of any crosswinds, as the respective signals travel along a perfectly vertical path.

For applications like two way range finding involving the relatively weak gravity field of Earth, the differences in travel time between the two directions almost completely cancel each other out (and researchers would be none the wiser). For example, the net difference between the two trips for this GPS test is only 85 picoseconds ( $8.5 \times 10^{-11}$  seconds).

### Revisiting Gravity Probe A

In 1976, a relativity experiment known as Gravity Probe A was conducted. [18] Its purpose was to test the time dilation of an object in the weaker gravitational field above Earth. The probe was carried by rocket to an altitude of 10,000 km, where it proceeded to fall back to Earth. In agreement with relativity predictions, the test showed that the probe experienced less time dilation than Earth-bound objects, and provided useful data for the GPS satellites that began to be constructed and launched into orbit shortly thereafter.

Even at the probe's apogee of 10,000 km, the rate of the flow is roughly 7,000 m/s, as given by Eq. (1) with  $a = 10,000$ . Even though this is significantly less than the flow at Earth's surface [See Eq. (5)], resulting in 'less' time dilation, a more dramatic result would be zero time dilation.

As the only condition where time dilation does not occur for an object is when it is motionless relative to the flow, another experiment similar to Gravity Probe A should be performed. The principle difference being that, instead of just letting the probe free fall from its apogee, accelerate it straight downward until its velocity (relative to Earth) matches the velocity of the flow (also relative to the Earth). Once the velocities are identical, disengage the thrusters and let the probe free fall from that point on. Since the probe will then be motionless relative to the flow (*i.e.*, in the motionless rest state), it will experience no time dilation.

For optimal effect and accuracy, the rocket's ascent trajectory will need to be configured such that the probe's descent trajectory will be along a sidereal line. The best (and possibly easiest) sidereal line would be in the direction of Earth's orbital path, which means the test would need to be carried out at dawn.

The time dilation factor for the probe will be zero (0), which is equivalent to the proper time of deep space. The time dilation factor for clocks on Earth's surface is  $6.967 \times 10^{-10}$ , as is given in Eq. (8) of the GPS satellite time dilation calculation at the outset of this paper.

**Flow-Affected Light Path**

An experiment to test the flow-affected path, which the signal is described as following in the Shapiro delay section, could be conducted by sending a space probe into high orbit around Mercury. The setup would be largely synonymous with that of Shapiro's experiment, in that the Earth, the Sun and the third body (Mercury in this case) would be in near superior conjunction.

The aim of this test would be to show the path taken by a signal sent from the probe. As such, have the probe start sending a countdown signal just as it is about to go behind the planet, with the countdown timed so that it reaches zero right when the planet would block/obscure any signal following the relativity predicted path. Nevertheless, have the probe continue sending the signal with the countdown going into negative numbers. It will turn out that the extended portion of the signal carrying the negative countdown numbers will be received for a short period of time because the flow affected path is arched (elongated) compared to the relativity predicted path. (See Fig. 14)

**Remarks**

In the second century, Ptolemy (Claudius Ptolemaeus) constructed a surprisingly accurate model of the solar system,[19] which was useful for predicting both the motions and future positions of the planets, even though he based it on a false premise. The scholars of his day thought that the solar system (and the universe for that matter) was geocentric.[20]

Laboring from this perspective, he had to compensate for what he didn't know - that the solar system is heliocentric. To make it work, he conceived that the planets were actually on the rims of epicycles, and added an offset equant.[19] Thus, the model was able to account for the retrograde motions of the planets. It was very accurate, causing it to be widely adopted and utilized for more than 1,300 years.[21] Today, Ptolemy's model stands as a classic example of the fact that just because something works, doesn't mean that it isn't based on a false premise.

When Einstein was formulating general relativity, he envisioned a curved space-time as a way of accounting for what were otherwise inexplicable observed behaviors. Like Ptolemy's model, relativity has certainly been shown to be accurate. But in envisioning a curved space-time, was Einstein simply compensating for what he didn't know - that space-time flows?

Gravitational flow is a single model covering the domains of both general and special relativity, and it does so without suffering from time dilation paradoxes or requiring tortured explanations of incongruous reference frames.

For perspective, Appendix D lists a summary of differences between relativity and gravitational flow.

**Appendix A. Orbital Precession Look-up Data**

Table 1: Time Dilation and Perihelion Precession Values

body	eccentricity	period	dilation in	dilation out	total	arc sec / Earth century
Mercury	0.20563	87.9691	0.163401	0.127326	0.80816	43.22
Venus	0.00675	224.701	0.199513	0.197902	0.80294	8.63
Earth	0.01671	365.256	0.235982	0.231295	0.95839	3.84
Mars	0.09331	689.971	0.304568	0.272227	1.33208	1.35
Icarus	0.82684	408.76	0.378768	0.106370	7.06686	9.38

Table 2. Minimalist Method Angles and Factors

eccentricity	angle	factor	body
0.0	13.6996308594	0.0000000000	
0.006755508	13.6996070052	0.0054485343	Venus
0.01	13.6995782849	0.0080653596	
0.01671123	13.6994835363	0.0134784207	Earth
0.02	13.6994197079	0.0161311438	
0.03	13.6991551993	0.0241977775	
0.04	13.6987844380	0.0322656862	
0.05	13.6983143844	0.0403309490	
0.06	13.6977222246	0.0484070366	
0.07	13.6970294783	0.0564813359	
0.08	13.6962278876	0.0645586263	
0.09	13.6953164699	0.0726393420	
0.093315036	13.6949899067	0.0753189627	Mars

eccentricity	angle	factor	body
0.10	13.6942941041	0.0807239200	
0.11	13.6931913361	0.0888128003	
0.12	13.6919193361	0.0969064267	
0.13	13.6905479738	0.1050052467	
0.14	13.6890677357	0.1131097123	
0.15	13.6874762575	0.1212188280	
0.16	13.6857490249	0.1293374117	
0.17	13.6839063411	0.1374615746	
0.18	13.6819383485	0.1455932422	
0.19	13.6798425084	0.1537328942	
0.20	13.6776160972	0.1664724963	
0.205630208	13.6763040459	0.1664724963	Mercury
0.21	13.6752561989	0.1700381062	

eccentricity	angle	factor	body
0.22	13.6727596968	0.1782046625	
0.23	13.6701232652	0.1863811973	
0.24	13.6673433593	0.1945682301	
0.25	13.6644237560	0.2027654303	
0.26	13.6613377904	0.2109759181	
0.27	13.6581038478	0.2191976636	
0.28	13.6547098468	0.2274320890	
0.30	13.6474221353	0.2439412909	
0.31	13.6435179054	0.2522172562	
0.32	13.6394325440	0.2605082810	
0.33	13.6351599596	0.2688149969	
0.34	13.6306936922	0.2771380519	
0.35	13.6260344633	0.2854775144	

eccentricity	angle	factor	body
0.36	13.6211522874	0.2938358606	
0.37	13.6160621731	0.3022120022	
0.38	13.6107483667	0.3106072614	
0.39	13.6052021842	0.3190223849	
0.40	13.5994144044	0.3274581431	
0.41	13.5933752316	0.3359153315	
0.42	13.5870742545	0.3443947718	
0.43	13.5805004019	0.3528973141	
0.44	13.5736418939	0.3614238385	
0.45	13.5664937542	0.3699748132	
0.46	13.6776160972	0.1664724963	
0.47	13.5512288497	0.3871565972	
0.48	13.5430977647	0.3957885222	

eccentricity	angle	factor	body
0.49	13.5346104305	0.4044493533	
0.50	13.5257494899	0.4131401971	
0.51	13.5164963704	0.4218622077	
0.52	13.5068311790	0.4306165897	
0.53	13.4967325852	0.4394046021	
0.54	13.4861776909	0.4482275625	
0.55	13.4751494132	0.4570865117	
0.56	13.4635986840	0.4659839161	
0.57	13.4515195458	0.4749202782	
0.58	13.4388736716	0.4838975371	
0.59	13.4256277744	0.4929173779	
0.60	13.4117458223	0.5019815779	
0.61	13.3971887469	0.5110920147	

eccentricity	angle	factor	body
0.62	13.3819141124	0.5202506752	
0.63	13.3658757403	0.5294596652	
0.64	13.3490232799	0.5387212202	
0.65	13.3313017179	0.5480377182	
0.66	13.3126508140	0.5574116933	
0.67	13.2930044500	0.5668458510	
0.68	13.2722898771	0.5763430868	
0.69	13.2504268405	0.5859065055	
0.70	13.2273265563	0.5955394446	
0.71	13.2028905126	0.6052455005	
0.72	13.1770090543	0.6150285594	
0.73	13.1495597066	0.6248928318	
0.74	13.1204051763	0.6348428936	

eccentricity	angle	factor	body
0.75	13.0893909519	0.6448837343	
0.76	13.0563424096	0.6550208124	
0.77	13.0210612890	0.6652601231	
0.78	12.9833213782	0.6756082767	
0.79	12.9428631790	0.6860725941	
0.80	12.8993872558	0.6966612225	
0.81	12.8525458600	0.7073832757	
0.82	12.8019322634	0.7182490081	
0.826837896	12.7649088200	0.7257675642	Icarus
0.83	12.7470670227	0.7292700309	
0.84	12.6873800425	0.7404595848	
0.85	12.6221868139	0.7518328891	
0.86	12.5506564187	0.7634075927	

eccentricity	angle	factor	body
0.87	12.4717676185	0.7752043714	
0.88	12.3842473388	0.7872477270	
0.89	12.2864823492	0.7995670876	
0.90	12.1763888435	0.8121983546	
0.91	12.0512134450	0.8251861476	
0.92	11.9072172947	0.8385871774	
0.93	11.7391501333	0.8524755348	
0.94	11.5393211638	0.8669514407	
0.95	11.2958281461	0.8821567390	
0.96	10.9888240416	0.8983049268	
0.97	10.5814437137	0.9157472565	
0.98	9.9923516633	0.9351495008	
0.99	8.9713025424	0.9581650753	

### Appendix B. Boundary-Value Calculations

The rigorous nature of scientific calculations requires that any result, intermediate or final, adhere to conventions regarding significant figures. The GPS satellite solution given near the outset of this paper does just that. However, there are situations where critical differences between very large numbers are so tiny that imposition of significant figures causes those critical differences to be lost. For example, compare the result in Eq. 17 with that in Eq. 19. In such cases, the calculations can instead be performed using boundary values.

Calculations using boundary values involves utilizing the highest and lowest values for each input value. For example, if a measurement value is given as 3.5, it means that the actual value is closer to 3.5 than 3.6 (on the high side), and closer to 3.5 than 3.4 (on the low side). As such, the upper boundary (limit) is 3.55, because the actual value cannot be higher. Similarly, the lower boundary is 3.45, because the actual value cannot be lower.

The process of determining the upper and lower boundaries is likewise carried out for all input values. For example, given input values of 3.5, 14.870 and 7.508E+6, the boundary values are 3.55 and 3.45, 14.8705 and 14.8695, and 7.5085E+6 and 7.5075E+6 respectively.

Since there are two boundary values for each of the three input values, the calculations need to be run 2<sup>3</sup> times: once for each unique combination of boundary values, as depicted in the following Matrix:

Boundary Values Matrix:

	Boundary 1	Boundary 2	Boundary 3
High	3.55	14.8705	7.5085E + 6
Low	3.45	14.8695	7.5075E + 6

Values Used in Eight Executions:

Execution	1	2	3	4	5	6	7	8
Boundary 1	H	L	H	H	H	L	L	L
Boundary 2	H	H	L	H	L	H	L	L
Boundary 3	H	H	H	L	L	L	H	L

Once all combinations of the boundary values have been run through the calculations, the highest and lowest resulting an-

swers are selected. The actual answer is guaranteed to be within the range of these two answers. Comparing the two answers, all leading digits that match (these are the significant figures) are retained, and all the other/trailing digits are discarded.

Performing the calculations in this manner allows as many trailing zeroes to be tacked on to the boundary values as needed – without compromising the validity of the calculations whatsoever. As an exercise, the GPS calculations were recalculated using boundary values, and the final result matched that of the traditional significant figures method.

The intermediate values shown in the minimalist method solution are simply midpoint values (at each step) between the highest and lowest boundary values executions.

### Appendix C. Example Calculations for MMX

Consider the 1887 Michelson-Morley Experiment, MMX.[22] Given Earth’s orbital velocity of 30 km/s and using white light with the 11.0 meter arm length interferometer Michelson and Morley constructed, they expected a 0.4 fringe pattern shift.

Note that ‘white’ light is not one of the colors of the visible spectrum (from 400 to 700 nanometers), but rather light composed of all the visible wavelengths simply appears as white. As such, the average visible wavelength of 550 nanometers is used in the following example solution.

As with the minimalist perihelion precession calculations, boundary calculations were used in this solution. Also note that the calculations presented are not meant to be a replica of how Michelson and Morley actually determined the expected fringe shift.

#### Set-up Data

Arm length  $l_{arm} = 11.0$  m [10]

Orbital velocity of Earth  $v_{Earth} = 30$  km/sec [11]

Wavelength of ‘white’ light  $\lambda = 5.50 \times 10^{-7}$  m

Light speed  $c = 288,792,458$  m/s [4]

#### Solution

Calculate the standard leg time ( $t_{leg}$ ). This is the time (in seconds) it would take the light beam to travel the distance of the

11.0 meter leg when it is perpendicular to the direction of Earth's orbital path:

$$t_{\text{leg}} = l_{\text{arm}} / c = 3.669205 \times 10^{-8} \text{ sec} \quad (47)$$

Calculate the headwind leg time ( $t_{\text{hw}}$ ). This is the time (in seconds) it would take the light beam to travel the distance of the 11.0 meter leg when it is in line with Earth's orbital path, and is headed in the same direction:

$$t_{\text{hw}} = l_{\text{arm}} / (c - v_{\text{Earth}}) = 3.669572 \times 10^{-8} \text{ sec} \quad (48)$$

Calculate the tailwind leg time ( $t_{\text{tw}}$ ). This is the time (in seconds) it would take the light beam to travel the distance of the 11.0 meter leg when it's in line with Earth's orbital path, but is headed in the opposite direction:

$$t_{\text{tw}} = l_{\text{arm}} / (c + v_{\text{Earth}}) = 3.668838 \times 10^{-8} \text{ sec} \quad (49)$$

Calculate the total standard time ( $t_{\text{tot}}$ ), for both the outbound and inbound legs:

$$t_{\text{tot}} = 2t_{\text{leg}} = 7.338410094 \times 10^{-8} \text{ sec} \quad (50)$$

Calculate the total 'wind' time ( $t_{\text{wind}}$ ), for both the outbound (into the aether wind) and inbound (away from the aether wind) legs:

$$t_{\text{wind}} = t_{\text{hw}} + t_{\text{tw}} = 7.338410167 \times 10^{-8} \text{ sec} \quad (51)$$

Calculate the net difference between the 'wind' time and standard time ( $t_{\text{dif}}$ ):

$$t_{\text{dif}} = t_{\text{wind}} - t_{\text{tot}} = 7.348574227 \times 10^{-16} \text{ sec} \quad (52)$$

Calculate the number of standard wavelengths per second ( $w_{\text{std}}$ )

$$w_{\text{std}} = c / \lambda = 5.450772 \times 10^{14} \lambda/\text{s} \quad (53)$$

Calculate the number of standard wavelengths for the arm length ( $\lambda_{\text{std}}$ ):

$$\lambda_{\text{std}} = t_{\text{tot}} \times w_{\text{std}} = 4.0 \times 10^7 \quad (54)$$

Calculate the number of 'wind' affected wavelengths for the arm length ( $\lambda_{\text{wind}}$ ):

$$\lambda_{\text{wind}} = t_{\text{wind}} \times w_{\text{std}} = 4.0000000400554 \times 10^7 \quad (55)$$

Calculate the total number of fringe band shifts possible:

$$\lambda_{\text{wind}} - \lambda_{\text{std}} = 0.4 \text{ fringe shifts} \quad (56)$$

The escape velocity at Earth's surface is only 11,191 m/s (Eq. 7), so an interferometer designed to detect the flow in the vertical plane would need to be very sensitive. For example, if a 532 nanometer laser were used, the device would need to have an effective arm length of 76.5 meters to produce an equivalent 0.4 fringe shift.

## Appendix D. Summary of Differences to Relativity

	Special Relativity	General Relativity	Gravitational Flow
Speed of Light in the Vacuum of Empty Space	The speed of light is constant, and independent of the motion of its source.	The speed of light is constant, and independent of the motion of its source.	The speed of light is constant, and independent of the motion of its source relative to the flow.
Speed of Objects	No object can achieve the speed of light.	No object can achieve the speed of light.	No object can achieve the speed of light relative to the flow. However, as the flow can travel faster than the speed of light relative to the cosmos, all objects can travel faster than the speed of light relative to the cosmos.
Reference Frames	All uniform motion is relative in the inertial frame.	All accelerated motion is relative in the non-inertial frame.	All motion is measured relative to the local flow, and the local flow is measured relative to the cosmos.
Motion Differentiation	No experiment can differentiate between uniform motion and motionlessness.	No experiment can differentiate between gravity and an equivalent amount of acceleration.	Interferometers can be used to differentiate between gravity and an equivalent amount of acceleration, and between uniform motion and motionlessness—all relative to the local flow.
Time Dilation	Time dilation is measured relative to the speed of light.	Time dilation is measured relative to the curvature of space-time.	Time dilation is measured relative to the local flow.
Zero Time Dilation	As time dilation is arbitrary between objects, any object can be assumed stationary to achieve zero time dilation.	N/A—Zero time dilation cannot be achieved in the presence of a sufficiently strong gravitational field.	Relative to the local flow, zero time dilation can be achieved anywhere in the universe, as objects only need to be in the motionless rest state—i.e., motionless relative to the local flow.

## References

- [1] R. Penrose (2004). *The Road to Reality: A Complete Guide to the Laws of the Universe*. Vintage Books. pp. 410-1. ISBN 978-0-679-77631-4.
- [2] CRC Handbook of Chemistry and Physics, 80th edition (1999). ISBN 0- 8493-0480-6.
- [3] R.A. Nelson. *The Global Positioning System. Via Satellite*, November 1999.
- [4] P.J. Mohr, B.N. Taylor, D.B. Newell (2008). "CODATA Recommended Values of the Fundamental Physical Constants: 2006" Rev. Mod. Phys. 80 (2): 663- 730.
- [5] C.F. Yoder (1995). T.J. Ahrens, ed. *Global Earth Physics: A Handbook of Physical Constants*. Washington: American Geophysical Union. p. 12.
- [6] N. Samama (2008). *Global Positioning: Technologies and Performance*. John Wiley & Sons. p. 65. ISBN 0-470-24190-X.
- [7] J.J. Spilker, Jr., B.W. Parkinson. *Global Positioning System: Theory and Applications*, Volume 1. p. 38. Progress in Astronautics and Aeronautics, Vol. 163. AIAA (1996).
- [8] I.I. Shapiro (1964). "Fourth Test of General Relativity". *Physical Review Letters* 13 (26): 789-791.
- [9] J. Mester (2006). "Experimental Tests of General Relativity". IHP Stanford University.
- [10] I.I. Shapiro, G.H. Pettengill, M.E. Ash, M.L. Stone, W.B. Smith, R.P. Ingalls, R.A. Brockelman (1968). "Fourth Test of General Relativity: Preliminary Results". *Physical Review Letters* 20 (22): 1265-1269.
- [11] P. Marmet, C. Couture. "Relativistic Deflection of Light Near the Sun Using Radio Signals and Visible Light". *Physics Essays*, Vol: 12, No: 1 March 1999. pp. 162-174.
- [12] R. Baum, W. Sheehan. "In Search of Planet Vulcan: The Ghost in Newton's Clockwork Universe". Plenum Press, 1997.

- [13] A.E.L. Davis. "The Mathematics of the Area Law: Kepler's successful proof in *Epitome Astronomiae Copernicanae* (1621)", *Archive for History of Exact Sciences* 57, 5 (2003).
- [14] W. Millar. "The Amateur Astronomer's Introduction to the Celestial Sphere". Cambridge University Press (2006). p. 164.
- [15] A.M. Steane. *Relativity Made Easy*. Oxford University Press (2012). p. 283.
- [16] P.M. Dauber, R. Muller. *The Three Big Bangs: Comet Crashes, Exploding Stars, and the Creation of the Universe*. Basic Books (1996). pp. 147-148.
- [17] S. Thornton, A. Rex. *Modern Physics for Scientists and Engineers*. Cengage Learning (2012). p. 24.
- [18] P.F.C. Vessot *et al.* Test of Relativistic Gravitation with a Space-Borne Hydrogen Maser. *Phys. Rev. Lett.* 45, 2081 (1980).
- [19] J. Evans (1984). "On the foundation and the probable origin of Ptolemy's equant". *American Journal of Physics* (52) 1080.
- [20] R.M. Larson. (2004). *Science in the Ancient World: An Encyclopedia*. ABC-CLIO. pp. 29-30.
- [21] M. Zeilik. *Astronomy: The Evolving Universe*. Cambridge University Press (2002). pp. 42-43.
- [22] A.A. Michelson, E. Morley. On the Relative Motion of the Earth and the Luminiferous Ether. *American Journal of Science*, 1887, 34 (203): 333-345.